Submitted as Communication to *Journal of the American Ceramic Society,* December 2009

Hertzian Indentation of a ZrB_2-30% SiC Ultra-High-Temperature Ceramic up to 800 °C in Air

Victor Zamora, Estíbaliz Sánchez-González, Angel L. Ortiz *,
Pedro Miranda, Fernando Guiberteau
Departamento de Ingeniería Mecánica, Energética y de los Materiales,
Universidad de Extremadura, Badajoz, Spain

Abstract

The contact mechanical properties of the ZrB_2-30% SiC ultra-high-temperature ceramic (UHTC) were studied from room-temperature up to 800 °C in air, by combining Hertzian indentation tests with finite element modelling. It was found that the elastic modulus and yield stress decrease with increasing temperature, especially above 600 °C. It was also found that the ZrB_2-30% SiC UHTC is "ductile" in the sense that its first damage mode is quasi-plasticity, followed by cone-cracking, and eventually by radial-cracking. However, its contact-damage resistance degrades as the temperature increases, again especially above 600 °C. Nevertheless, it is highly damage-tolerant because the critical loads for radial-cracking are one order of magnitude greater than these for quasi-plasticity. This is the first report on the temperature-dependence of the Hertzian indentation of UHTCs, whose study is necessary if they are to be used in aerospace applications.

Keywords: ZrB_2; Hertzian indentation; ultra-high-temperature ceramics; contact-mechanical properties.

* Corresponding author:
Angel L. Ortiz
Phone: +34 924289600 Ext: 86726
Fax: +34 924289601
E-mail: alortiz@materiales.unex.es

1. Introduction

Ceramics based on transition-metal borides, carbides, and nitrides —commonly known as ultra-high-temperature ceramics (UHTCs)— are promising candidates for applications at extreme temperatures in very hostile environments, one of the which is the thermal protection of the wing leading edges and nosetips of future hypersonic flight vehicles (including sub-orbital and earth-to-orbit vehicles for rapid global and space access missions) [1-4].

However, despite intense recent research efforts, UHTCs are still far from being utilized routinely as hypersonic aerosurfaces because some do not have the required set of properties, and in others the microstructure-processing-property relationship is still not well understood. This latter is particularly true of the high-temperature mechanical properties in the creep and pre-creep regimes because most studies on UHTCs have centred on investigating lower-temperature sintering, resistance to oxidation and thermal shock, and room-temperature mechanical properties [3-4]. That there is only sparse information available for the pre-creep regime, and that this is mostly concentrated on flexure strength, is especially surprising because it is in this temperature range that UHTCs would be required to work in most practical applications. Even in aerospace applications where UHTCs may reach creep temperatures, mechanical stresses are most likely to occur during the heating and cooling cycles. In this context, pre-creep contact mechanical properties have to be considered as important factors in the design of UHTCs for aerospace applications, as has been learned from the disaster of the space shuttle Columbia— which was the result of the damage caused by the contact of a detached piece with the thermal protection system of the left wing's leading edge [5]. An ideal method of evaluating pre-creep contact-mechanical properties is by the Hertzian testing methodology, which enables one to determine the entire evolution of the contact damage with increasing contact pressure as a function of temperature.

Despite the unquestionable importance of studying the contact-mechanical properties of UHTCs to ensure their mechanical integrity under service conditions, there has as yet been no research effort in this direction. The present study seeks to address this deficiency, and is indeed the first attempt to systematically investigate the Hertzian-indentation response of UHTCs as a function of temperature in air. In particular, a prototypical ZrB_2-30% SiC UHTC was characterized mechanically by Hertzian testing at moderate temperatures (25–800 °C) in air.

While this temperature range was dictated by the complexity of testing air-sensitive ceramics, it is nonetheless the regime of greatest interest for contact-resistance aerospace applications.

2. Experimental Procedure

A powder batch was prepared, containing 70 vol.% of micrometre (2-3 μm) ZrB_2 powder (Grade B, H.C. Starck, Goslar, Germany) and 30 vol.% of submicrometre (0.5 μm) α-SiC powder (UF-15, H.C. Starck, Goslar, Germany). The powder batch was attrition milled (01-HD, Union Process, Akron, OH, USA) for 3 h at 600 rpm using WC/Co balls (6.7 mm diameter) with a charge ratio of 24:1 to reduce particle size and promote intimate mixing. The milled powder was hot-pressed (HP20-3560-20, Thermal Technology LLC, Santa Rosa, CA, USA) at 1900 °C for 1 h at 30 MPa pressure. More details of the hot-pressing protocol are given elsewhere [6]. The surfaces of the hot-pressed samples were polished to a 1 μm finish and sputter-coated with a thin (~5 nm) metallic film for its microstructural characterization by scanning electron microscopy (SEM; S-3600N, Hitachi, Japan) and mechanical characterization by Hertzian testing [7].

Hertzian contact tests were performed in air in the temperature range 25–800 °C using a universal testing machine (AG-IS 100 kN, Shimadzu Corp., Kyoto, Japan) equipped with a split furnace. The indentation sequences were carried out at a constant crosshead speed of 0.05 mm/min over the peak load range 50–7000 N, using a Si_3N_4 half-sphere of 3 mm radius (r) as indenter. Prior to testing, the specimens were heated to the desired temperature at 6 °C/min and soaked for 1 h in order to ensure thermal equilibrium. The contact radius (a) for each peak load (P) was measured after each test sequence using an optical microscope, and used to construct the indentation stress−strain curves (*i.e.*, the plots of $p_0=P/\pi a^2$ versus a/r) [8].

Young's modulus (E) was calculated directly from the linear region of the indentation stress–strain curve using the Hertzian relation for elastic contacts [8,9]

$$p_0 = \frac{4/3\pi}{\left(1-\nu^2\right)/E + \left(1-\nu'^2\right)/E'} \frac{a}{r} \qquad (1)$$

where ν is Poisson's ratio, and the primes indicate indenter properties [10]. The error in E was calculated by error propagation in Eq. (1).

The strain-hardening coefficient (n) and the yield stress (Y) were determined by reproducing the entire indentation stress–strain curve by finite element modeling (FEM) using the following constitutive uniaxial elasto-plastic model [11]:

$$\sigma = E\varepsilon \qquad (\sigma < Y) \tag{2a}$$

$$\sigma = Y(E/Y)^n \varepsilon^n \qquad (\sigma < Y) \tag{2b}$$

the validity of which has been confirmed in earlier studies [7,10,12,13]. The errors in n and Y are their standard deviations determined by FEM. The critical loads for initiation of quasi-plasticity (P_Y) were subsequently calculated from the expression [8,9]:

$$P_Y = \frac{9}{16}\left(\frac{1-\nu^2}{E} + \frac{1-\nu'^2}{E'}\right)^2 (\pi 1.1Y)^3 r^2 \tag{3}$$

The error in P_Y was calculated by error propagation in Eq. (3). The critical loads for initiation of fracture in the form of radial cracks (P_R) and ring/cone (P_C) cracks were taken as the lowest applied load at which such a cracking mode was observed during the examination of the surface damage with the optical microscope. The error in P_C and P_R was considered to be the difference between the load at which cracking was observed and the preceding load in the test sequence.

Finally, the room-temperature hardness and toughness were determined by Vickers-indentation tests (load 98 N, indentation load rate 40 μm/s, and dwell time 20 s) using standard formulae [14,15].

3. Results

Figure 1 shows a representative SEM micrograph of the room-temperature fracture surface of the ZrB_2-30% SiC UHTC in the as-processed condition. As can be seen, it has the usual microstructure of submicrometre SiC grains dispersed homogeneously in a matrix of micrometre ZrB_2 grains. The room-temperature hardness and toughness measured by Vickers testing are 20.7±0.5 GPa and 3.6±0.1 $MPa \cdot m^{0.5}$, respectively, which are standard values for ZrB_2-30% SiC UHTCs.

Figure 2 shows the indentation stress-strain curves for the ZrB_2-30% SiC UHTC from 25 °C to 800 °C, which is the maximum temperature at which the imprint size could be accurately measured due to extensive surface oxidation. As can be observed, this UHTC exhibits the Hertzian curves typical of other polycrystalline ceramics, that is, an initial linear stretch at low contact pressures that corresponds to the elastic deformation regime, followed by a non-linear

stretch that corresponds to the quasi-plastic deformation regime. At high contact pressures the curves tend towards an asymptotic limit, which is the corresponding Meyer's hardness. It is also observed in Fig. 2 that as the temperature increases the slope of the linear stretch, the contact pressure for the onset of quasi-plastic deformation, and the asymptotic limit all diminish, indicating that the elastic modulus, the yield stress, and the hardness of the UHTC decrease with increasing temperature.

Figure 3 shows the elastic modulus and yield stress of the ZrB_2-30% SiC UHTC as a function of temperature. As can be observed, the elastic modulus first decreases slowly up to ~ 600 °C, and then the fall accelerates. The yield stress, however, exhibits first a continuous decrease to ~ 600 °C, then drops, and finally flattens out. The strain hardening, on the contrary, was found to be temperature-independent, and as low as 0.17±0.02.

Figure 4 shows the critical loads for initiation of quasi-plasticity and fracture (cone and radial cracking), as a function of temperature. As can be observed, the critical load for quasi-plasticity (P_Y) first decreases from 673 N down to 381 N with increasing temperature up to 600 °C, then falls abruptly to 233 N at 700 °C to stabilize or continue declining slowly. The critical load for cone cracking also seems to fall at 700 °C, although the large experimental errors do not exclude a possible continuous fall from room-temperature. The critical load for radial cracking exhibits the same trend with temperature as P_Y, first decreasing continuously from more than 8000 N at 25 °C down to 4500 N at 600 °C, then falling abruptly to 2000 N at 700 °C, and finally decreasing again more slowly. It is interesting to note that critical loads for the onset of the different damage modes follow the sequence $P_Y < P_C << P_R$, and that the difference between P_C and P_Y increases with increasing temperature.

4. Discussion

We have investigated the Hertzian-indentation response of the ZrB_2-30% SiC composite from room-temperature up to 800 °C, representing the first study of this type on a UHTC. At 900 °C the borosilicate glass that forms the external layer of the oxide scale starts to flow under the high pressures applied in the Hertzian tests, making it difficult to measure the contact area. In any case, the fact that the maximum testing temperature was only 800 °C cannot be interpreted as a serious limitation of the method because in aerospace applications impacts are more likely to occur under the high aerodynamic forces developed during launch and first moments of ascent,

when the temperature of the UHTCs is not very high yet. Later during the flight to orbit and re-entry into the Earth's atmosphere surface oxidation and wear become more important issues than contact damage.

It has been observed that the elastic modulus of the ZrB_2-30% SiC composite first decreases slightly up to 600 °C, and then more rapidly (see Fig. 3). The initial moderate fall is the typical elastic modulus dependence on temperature, $E = E_0(1 - aT/T_m)$ where T_m is the melting temperature [16,17]. The accelerated fall above 600 °C is attributed to the activation of reversible grain boundary sliding [10,12,16,18,19]. Oxidation of the ZrB_2-30% SiC UHTC could also contribute in part to this fall because the so-formed ZrO_2 and SiO_2 have lower elastic modulus than ZrB_2 and SiC, respectively. However, this oxidation would represent only a minor contribution because even in the most hostile oxidation condition the thickness of the oxide scale is less than 5% of the thickness of elastically-deformed bulk zone.

The yield stress dictates the onset of quasi-plastic deformation, which is proposed to occur by shear-faulting along the weak ZrB_2-SiC interfaces because the large thermal expansion mismatch between the ZrB_2 and SiC grains generates residual stresses as high as 4.2 GPa at the ZrB_2-SiC interfaces [3]. The decreasing yield stress (see Fig. 3) simply reflects that the stress threshold for generating quasi-plastic damage decreases with increasing temperature because the thermal energy available is greater. Above 600 °C, grain boundary degradation is believed to contribute to the accelerated fall of the yield stress, although this expectation remains to be confirmed by experiments.

As the temperature increases, the asymptotic limit of the Hertzian curves also fall significantly (see Fig. 2), indicating a marked drop in the hardness. This softening is linked to the fall of the yield stress as the strain-hardening parameter is temperature-independent. The strain-hardening capability is low (0.17±0.02), which can be considered as a good attribute of the ZrB_2-30% SiC UHTC as high strain-hardening values are typically accompanied by greater susceptibility to fracture.

Let us now compare the load conditions to activate the different contact damage modes. The ZrB_2-30% SiC UHTC exhibits "ductile" contact behaviour in the whole temperature range examined in the sense that the first damage mode is always quasi-plasticity, not fracture (see Fig. 4), a trend that is more evident as the temperature increases. This is an important attribute for any UHTC, as it indicates a certain capacity of dissipating mechanical energy during contact without

macro-crack generation. The critical load for quasi-plasticity, however, decreases with increasing temperature. This is explained considering simply that P_Y depends on the yield stress (Y) and elastic modulus (E) as $P_Y \propto Y^3/E^2$ [8], and that Y and E decrease with temperature as plotted in Fig. 3. The critical load for cone-cracking also decreases with increasing temperature above 600 °C. This suggests that the toughness (K_{IC}) of ZrB_2-30% SiC UHTC decreases appreciably above 600 °C, as P_C satisfies the expression $P_C = 8.63 \cdot 10^3 K_{IC}^2 r/E$ [8] and E (see Fig. 3) decreases with temperature. Indeed, estimates performed using this expression indicate that K_{IC} decreases slowly from 3.6 MPa·m$^{0.5}$ at room-temperature down to 3.3 MPa·m$^{0.5}$ at 600 °C, and then drops to 2.7 and 2.5 MPa·m$^{0.5}$ at 700 and 800 °C, respectively— note that the toughness calculated for room-temperature is consistent with the 3.6±0.1 MPa·m$^{0.5}$ determined directly by Vickers indentation, which lends strong credence to the toughness calculations. Assuming crack deflection at the ZrB_2-SiC interfaces, which is the case at room temperature [21], this sudden fall in K_{IC} suggests again that these interfaces degrade above 600 °C. The "indentation strength" has also been calculated from the critical loads for cone-cracking, using the expression $\sigma = (1-2\nu)P_C/(2\pi a^2)$ [22]. In doing this, it is found that the ZrB_2-30% SiC UHTC retains a 91% of its room-temperature "indentation strength" of 1914±150 MPa up to 600 °C, and as much as a 72% at 800 °C. While this reduction in strength has also been observed in flexure tests [3,4], the "indentation strength" values are 2-3 times greater than the more typical bending strength values because of the differences in the stress fields and deformation modes under Hertzian indentation tests and the 4- or 3-point bending tests. Finally, it is also noted in Fig. 4 that P_C and P_Y curves split with increasing temperature, which can be explained with the input of the trends of K_{IC}, E and Y into the expressions $P_C \propto K_{IC}^2/E$ and $P_Y \propto Y^3/E^2$. This splitting ensures that quasi-plasticity will continue to be the first damage mode at higher temperatures.

With respect to the critical load for radial-cracking, it also decreases with increasing temperature but is always much higher than P_Y. This is expected because radial cracks originate due to the coalescence and growth of the microcracks nucleated at the weak ZrB_2-SiC interfaces (*i.e.*, quasi-plastic damage), and P_Y decreases with increasing temperature. The important finding is that P_R is one order of magnitude greater than P_Y (*i.e.*, than the critical load first damage mode), which indicates clearly that the ZrB_2-30% SiC UHTC is highly damage-tolerant. This is doubtless an important attribute of the ZrB_2-30% SiC UHTC because radial-cracking can cause

catastrophic failure, and therefore P_R dictates the maximum load for ensuring mechanical integrity in service. Note that although cone-cracking occurs well before radial-cracking, this damage mode is not likely to cause failure except under cyclic loading conditions— which is unlikely to occur in aerospace applications.

4. Conclusions

We have studied, for the first time, the elasto-plastic properties and contact damage evolution of an UHTC, in particular ZrB_2-30% SiC, as a function of temperature in air up to 800 °C, using to that end Hertzian indentation tests together with FEM. The elastic modulus and yield stress decrease with increasing temperature, while the strain-hardening is constant. The critical loads for onset of contact damage also decrease in general with increasing temperature, and follow the sequence $P_Y < P_C << P_R$ which indicates that the ZrB_2-30% SiC UHTC is "ductile" and damage-tolerant. Above 600 °C there occurs an important degradation of the contact mechanical properties, which we would attribute to weakening of the grain boundaries although this requires experimental confirmation. Finally, it is anticipated that systematic application of this method will help identify processing guidelines with which to make UHTCs highly contact-resistant for their use in aerospace applications.

Acknowledgements This work was supported by the Ministerio de Ciencia y Tecnología (Government of Spain) under Grant N° MAT 2007-61609.

References

1) M.M. Opeka, I.G. Talmy, and J.A. Zaykoski, "Oxidation-Based Materials Selection for 2000°C+ Hypersonic Aerosurfaces: Theoretical Considerations and Historical Experience," J. Mater. Sci., 39 [19] 5887–904 (2004).
2) D.M. Van Wie, D.V.Jr. Drewry, D.E. King, and C.M. Hudson, "The Hypersonic Environment: Required Operating Conditions and Design Challenges," J. Mater. Sci., 39 [19] 5915–24 (2004).
3) W.G. Fahrenholtz, G.E. Hilmas, I.G. Talmy, and J.A. Zaykoski, "Refractory Diborides of Zirconium and Hafnium," J. Am. Ceram. Soc., 90 [5] 1347–64 (2007). See also references therein.
4) S.-Q. Guo, "Densification of ZrB_2-Based Composites and their Mechanical and Physical Properties: A Review," J. Eur. Ceram. Soc., 29 [6] 995–1011 (2009). See also references therein.
5) Reports from the Columbia Accident Investigation Board, available at NASA Web site http://caib.nasa.gov/news/report/default.html
6) A. Rezaie, W.G. Fahrenholtz, and G.E. Hilmas, "Evolution of Structure during the Oxidation of Zirconium Diboride–Silicon Carbide in air up to 1500 °C," J. Eur. Ceram. Soc., 27 [6] 2495–501 (2007).
7) E. Sánchez-González, P. Miranda, J.J. Meléndez-Martínez, F. Guiberteau, A. Pajares, and B.R. Lawn, "Application of Hertzian Tests to Measure Stress-Strain Characteristics of Ceramics at Elevated Temperatures," J. Am. Ceram. Soc., 90 [1] 149–53 (2007).
8) B. R. Lawn, "Indentation of Ceramics with Spheres: A Century after Hertz," J. Am. Ceram. Soc., 81 [8] 1977–94 (1998).
9) K.L. Johnson, Contact Mechanics. Cambridge Univ. Press, Cambridge, UK, 1985.
10) E. Sánchez-González, P. Miranda, F. Guiberteau, and A. Pajares, "Effect of Temperature on the Pre-Creep Mechanical Properties of Silicon Nitride," J. Eur. Ceram. Soc., 29 [12] 2635-41 (2009).
11) P. Lüdwig, Element der Technologischen Mechanik. Springer, Berlin, 1909.
12) E. Sánchez-González, P. Miranda, J.J. Meléndez-Martínez, F. Guiberteau, and A. Pajares, "Temperature Dependence of Mechanical Properties of Alumina up to the Onset of Creep," J. Eur. Ceram. Soc., 27 [11] 3345-9 (2007).

13) E. Sánchez-González, P. Miranda, J.J. Meléndez-Martínez, F. Guiberteau, and A. Pajares, "Contact Properties of Yttria Partially Stabilized Zirconia up to 1000ºC," J. Am. Ceram. Soc., 90 [11] 3572-7 (2007).

14) B. R. Lawn, Fracture of Brittle Solids, 2nd edition, Cambridge University Press, Cambridge, U.K., 1993.

15) G. R. Anstis, P. Chantikul, D. B. Marshall, and B. R. Lawn, "A Critical Evaluation of Indentation Techniques for Measuring Fracture Toughness: I. Direct Crack Measurements," J. Am. Ceram. Soc., 64 [9] 533-38 (1981).

16) J. B. Wachtman Jr., and D. G. Lam Jr., "Young's Modulus of Various Refractory Materials as a Function of Temperature," J. Am. Ceram. Soc., 42 [5] 254-60 (1959).

17) R. G. Munro, "Analytical Representations of Elastic Moduli Data with Simultaneous Dependence on Temperature and Porosity," J. Res. Natl. Inst. Stand. Technol., 109 [5] 497-503 (2004).

18) G. Roebben, R. G. Duan, D. Sciti, and O. Van der Biest, "Assessment of the High Temperature Elastic and Damping Properties of Silicon Nitrides and Carbides with the Impulse Excitation Technique," J. Eur. Ceram. Soc., 22 [14-15] 2501-9 (2002).

19) R. J. Bruls, H. T. Hintzen, G. deWith, and R. Metselaar, "The temperature Dependence of the Young's modulus of $MgSiN_2$, AlN and Si_3N_4," J. Eur. Ceram. Soc., 21 [3] 263-8 (2001).

20) T. A. Parthasarathy, R. A. Rapp, M. Opeka, and R. J. Kerans, "A Model for the Oxidation of ZrB_2, HfB_2 and TiB_2," Acta Mater., 55 [17] 5999-6010 (2007).

21) A. Rezaie, W. G. Fahrenholtz, and G. E. Hilmas, "Effect of Hot Pressing Time and Temperature on the Microstructure and Mechanical Properties of ZrB_2–SiC," J. Mater. Sci., 42 [8] 2735-44 (2007).

22) H. Chai, and B. R. Lawn, "Fracture Mode Transitions in Brittle Coating Layers on Compliant Substrates as a Function of Thickness," J. Mater. Res., 19 [6] 1752-61 (2004).

Figure Captions

Figure 1. SEM micrograph of the room-temperature fracture surface of the ZrB_2-30% SiC UHTC. In general, the larger grains are ZrB_2 and the smaller grains are SiC.

Figure 2. Indentation stress–strain curves of the ZrB_2-30% SiC UHTC at temperatures in the range 25–800 °C. Points are the experimental data, and solid curves the FEM fits. The error bars are lower than the point size.

Figure 3. Elastic modulus (E) and yield stress (Y) of the ZrB_2-30% SiC UHTC as a function of temperature in the range 25–800 °C. The E and Y values and their errors were evaluated as described in the experimental section. The solid lines are guides to the eye.

Figure 4. Critical load for the initiation of quasi-plasticity, cone-cracking, and radial-cracking in the ZrB_2-30% SiC UHTC as a function of temperature in the range 25–800 °C. The P_Y, P_C, and P_R values and their errors were evaluated as described in the experimental section. The solid lines are guides to the eye, and the dashed lines denote abrupt falls. The doted line indicates that P_R was greater than 8000 N at room temperature, and was therefore not measured.

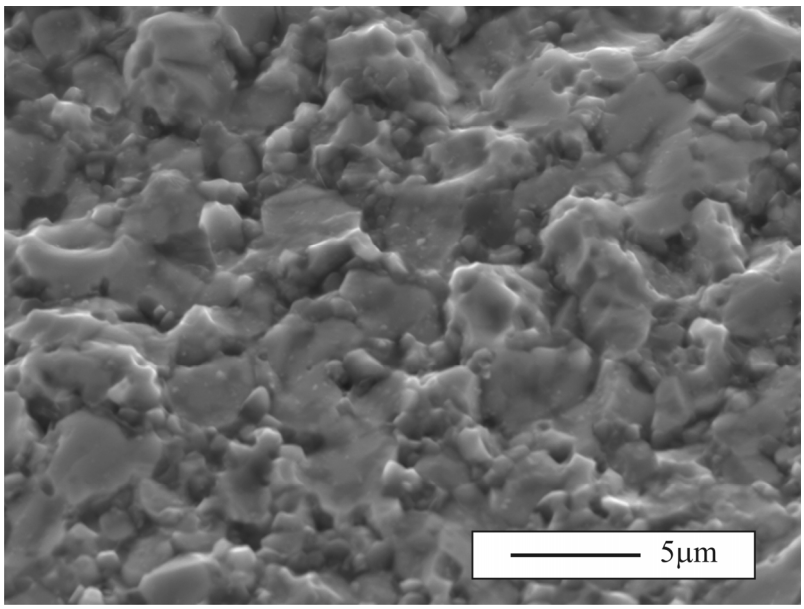

Figure 1

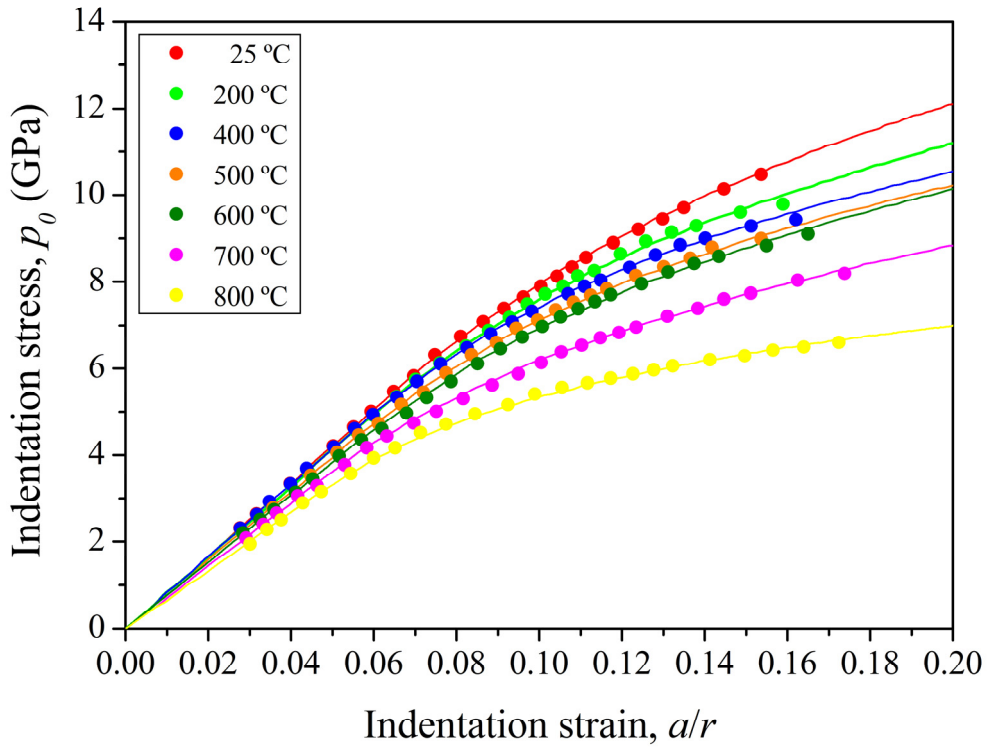
25 ºC
200 ºC
400 ºC
500 ºC
600 ºC
700 ºC
800 ºC
Indentation stress, p_0 (GPa)
Indentation strain, a/r
0
2
4
6
8
10
12
14
0.00
0.02
0.04
0.06
0.08
0.10
0.12
0.14
0.16
0.18
0.20

Figure 2

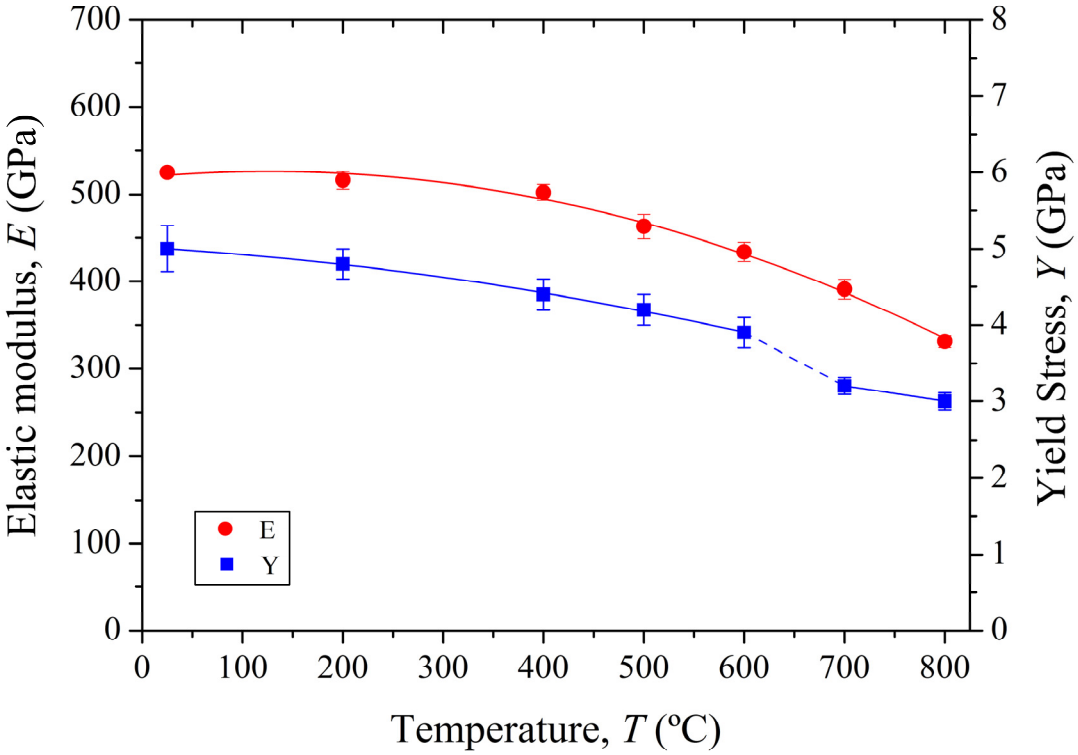
Elastic modulus, E (GPa)
Yield Stress, Y (GPa)
Temperature, T (ºC)
E
Y
0
100
200
300
400
500
600
700
800
1
2
3
4
5
6
7
8

Figure 3

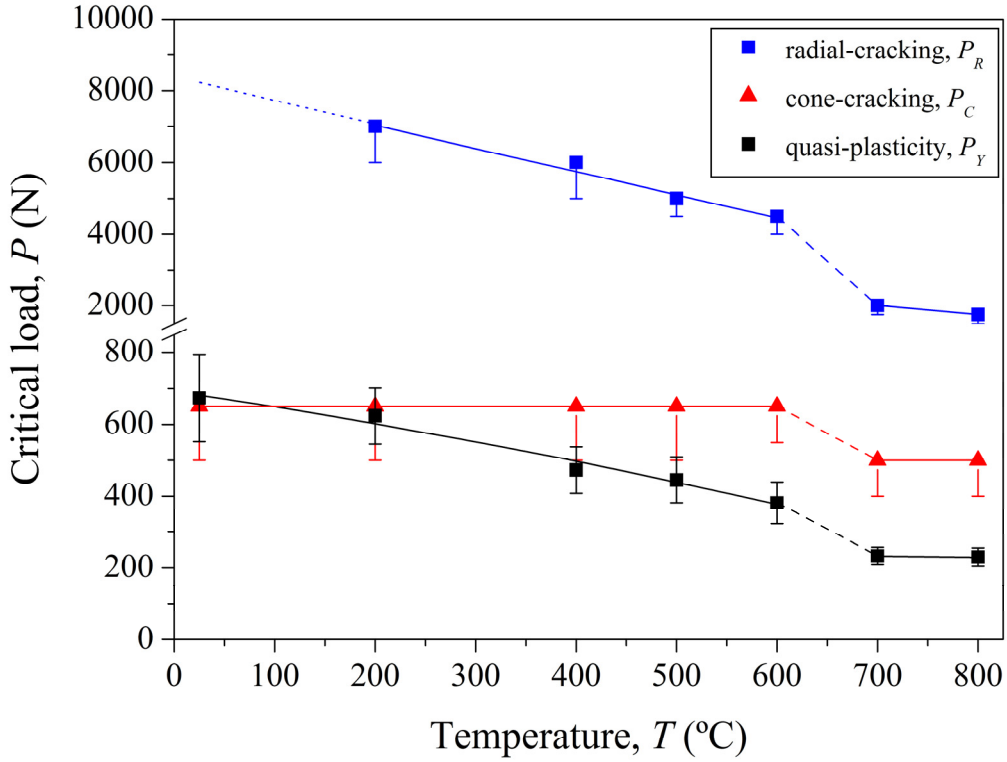
Critical load, P (N)
Temperature, T (°C)
radial-cracking, P_R
cone-cracking, P_C
quasi-plasticity, P_Y
10000
8000
6000
4000
2000
800
600
400
200
0
0
100
200
300
400
500
600
700
800

Figure 4